Jpn. J. Appl. Phys. Vol. 39 (2000) pp. 1920–1925
Part 1, No. 4A, April 2000
©2000 The Japan Society of Applied Physics

Development of Photochemical Analysis System for F_2-Excimer Laser Lithography Processes

Atsushi SEKIGUCHI*, Mikio KADOI, Yasuhiro MIYAKE and Toshiharu MATSUZAWA
Litho Tech Japan Corporation, Kawaguchi, Saitama 332-0034, Japan

(Received September 28, 1999; accepted for publication January 21, 2000)

A system for photochemical analysis of F_2-excimer laser lithography processes has been developed. The system, VUVES-4500, consists of 3 units: (1) an exposure and bake unit that uses the F_2-excimer laser to carry out a flood exposure and then post-exposure bake (PEB), (2) a unit for measurement of the development rate of photoresists, and (3) a simulation unit that utilizes PROLITH of profile simulation software to calculate the resist profiles and process latitude using the measured development rate data. With this system, preliminary evaluation of the performance of F_2-Excimer laser lithography can be performed without the use of a lithography tool capable of imaging and alignment. Profiles for 150 nm lines are simulated for the PAR-101 resist (manufactured by Sumitomo Chemical) and the SAL-601 resist (manufactured by Shipley), a chemically amplified resist that has sensitivity at the F_2-excimer laser wavelength. The simulation successfully predicts the resist behavior. Thus it is confirmed that the system enables efficient evaluation of the performance of F_2-excimer laser lithography processes.

KEYWORDS: chemically amplified resist, lithography simulation, F_2-excimer laser, resist development rates, exposure tool, homogenizer optical system

1. Introduction

In developing new resists, ordinarily a projection printing tool (a "stepper") capable of direct evaluation of the resolving properties and process tolerance is thought to be necessary.[1] However, work to develop a stepper for use with F_2 excimer lasers has just begun, and it is thought that considerable time will be needed before practical F_2 excimer laser steppers become available. In addition, resists are needed in order to assess the lens aberrations and resolution of the stepper during development, i.e., stepper development and resist development have a chicken-and-egg relationship.[2] Thus in order to accelerate stepper development, progress must be made in developing resist materials. Given this situation, there is a need for a system for evaluating new resists which dose not require a stepper. We have used lithography simulation to develop the VUVES-4500 vacuum ultraviolet excimer laser process evaluation system for photochemical analysis of new F_2 excimer laser processes without the use of a stepper.

Using this new system, we have studied the possibility of applying two existing resists to F_2 excimer laser exposure: PAR-101 ArF (193 nm) resist (positive, Sumitomo Chemical),[3] and SAL-601 electron-beam resist (negative, Shipley).[4] Herein we report our results.

2. System Configuration

VUVES-4500 consists of the following three base units.

(1) An exposure unit which uses F_2 excimer laser light for resist exposure, and also performs post-exposure baking (PEB) and cooling
(2) A unit for measurement and analysis of resist development rates for different exposure doses
(3) A simulator unit which employs the accumulated development data in numerical calculation of resist profiles and process margins

2.1 *Exposure and baking unit*

The F_2 excimer laser exposure, PEB and cooling unit consists of an F_2 excimer laser light source, optical system, exposure stage, PEB baking furnace, cooling plate, and wafer transfer robot. Figure 1 is an external view of the exposure and baking unit. The 157 nm laser light leaving the laser light source passes through an electronic shutter and is broadened by a beam expander lens. It then passes through a two-stage optical system with an array of 25 homogenizers (5 × 5) and is formed into a parallel ray, before passing through a collimator and impinging on the resist. The homogenizer optical system must efficiently pass laser light at 157 nm, and so it employs CaF_2. Throughout the entire optical path, all air is replaced by N_2. The exposure area is an open frame 8 mm per a side; in-plane uniformity within the exposed area is within ±5%. Figure 2 shows the results of optical path simulations

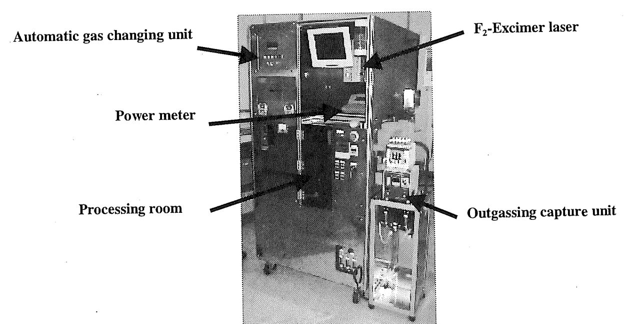

Fig. 1. External view of the VUVES-4500 system.

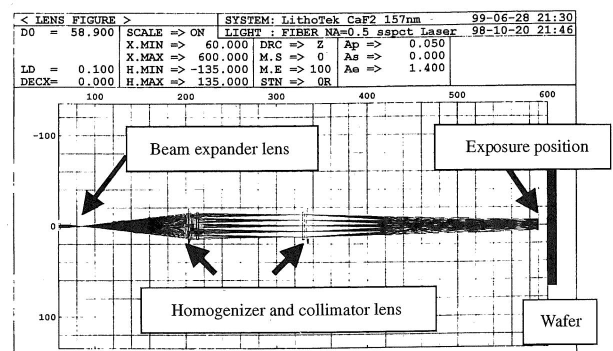

Fig. 2. Simulation result of locus for 157 nm light ray.

*E-mail: jun@ltj.co.jp

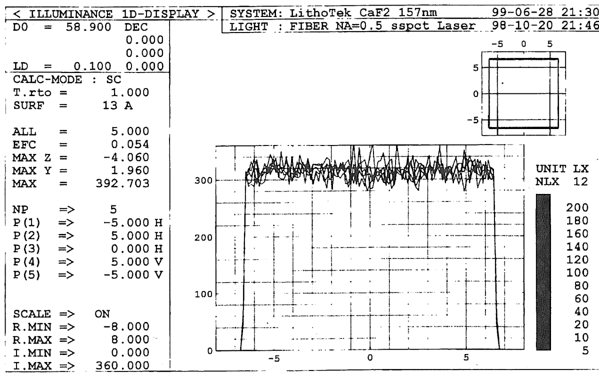

Fig. 3. Simulation result of pile on wafer for 157 nm light ray.

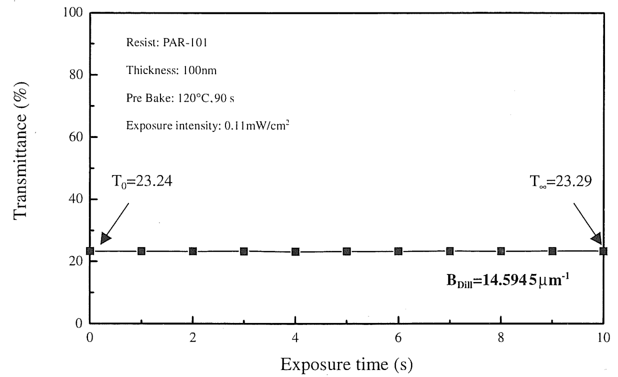

Fig. 4. Measured B_{Dill} parameter of PAR-101 by using VUVES-4500.

for the homogenizer optical system. Figure 3 shows simulated results for image formation on the wafer by light which has been split by the homogenizer lenses after passing through the homogenizer optical system. The exposure dose is controlled by placing a half-mirror in the optical path and monitoring the exposure energy *in situ*. The exposure dose can be set in the range of 0.01 to 500 mJ/cm^2, varied in 0.01 mJ/cm^2 steps. When exposure is completed, the robot transports the sample to the load/lock PEB baking furnace. The PEB baking furnace is positioned within the exposure system, and the air along the wafer transport line can be replaced using a chemical mica filter, so as to ensure an absolute minimum amine contaminants in the atmosphere (post exposure delay effect) between the completion of exposure and PEB. And by adopting a load/lock-type PEB baking furnace, any diffusion of outgassing during PEB within the exposure area can be prevented.

When PEB is completed, the transfer robot carries the sample to the cooling plate for cooling. Immediately after PEB the wafer is quickly cooled, so that superfluous deprotection reaction is suppressed. The time from PEB until cooling can be freely adjusted, so that the effect of the superfluous deprotection reaction can be studied.

A power sensor for measurement of transmittance was embedded in the exposure stage. By this means the transmittance of the resist material can be measured. The procedure for transmittance measurement is as follows. First, an MgF_2 substrate with no resist applied is placed on the exposure stage and irradiated with 157 nm laser light to calibrate the system. The transmittance at this time is taken to be 100%. Next, a sample composed of resist applied to an MgF_2 substrate is placed on the stage, and the transmittance of the resist material is measured. By substituting the transmittance thus obtained into eq. (1), the Dill *B* parameter[5] can be determined. Figure 4 shows an example of PAR-101 transmittance measurements and determination of the Dill *B* parameter.

$$B = -\left(\frac{1}{d}\right) \cdot \ln(T_\infty). \qquad (1)$$

Here, B is the Dill B parameter (μm^{-1}), d is resist thickness (μm), T_∞ is transmittance due to bleaching.

2.2 *Unit for measurement and analysis of resist development characteristics*

This unit contains a resist development analyzer[6] developed by us. The development rate of the resist is measured by shining monochromatic light on a thin film of the resist during development. When monochromatic light is incident on the resist film during development, the light reflected from the film surface interferes with the light reflected from the substrate surface. As the film thickness changes with development, the reflection intensity is observed to vary sinusoidally. By using the Dill theory of interference in thin films, the obtained interference waveform can be converted into a development rate.[7] Figure 5 shows measurement results for light reflected from PAR-101 irradiated with F_2 excimer laser light. The film thickness is 300 nm. Ordinarily at this film thickness, there are at least three fringe peaks, as in the theoretical waveform shown in the figure; but as Fig. 5 indicates, no fringe peaks appear, and there is only a monotonic increase. The cause of this is thought to be that, instead of the development proceeding layer by layer, irregular development in microscopic areas occurs, so that the monitoring light is scattered at the development interface.[8] Thus the usual Dill thin film interference theory cannot be applied to obtain the development rate in a resist film using reflected light data. Hence a method was proposed for predicting the depth-direction development rate profile by calculating the accumulated energy disteribution in the resist film.[9] This method is described below.

From Fig. 5, the so-called breakthrough time, at which the resist film has completely disappeared, can easily be determined (the breakthrough point in Fig. 5). Thus, the average development rate from the start of development until the resist completely disappears can also be determined. Using the measured value of the Dill *B* parameter discussed in the

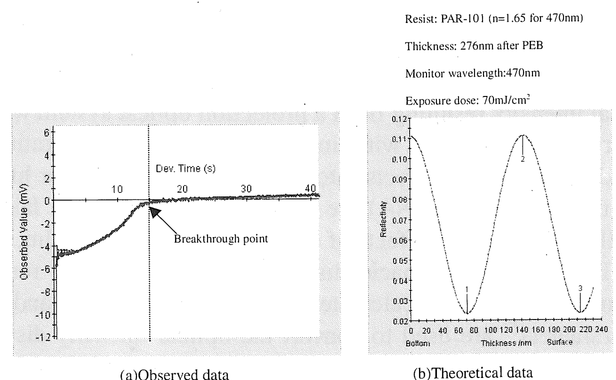

Fig. 5. Reflected signal obtained during the development reaction and theory of reflect intensity in depth direction.

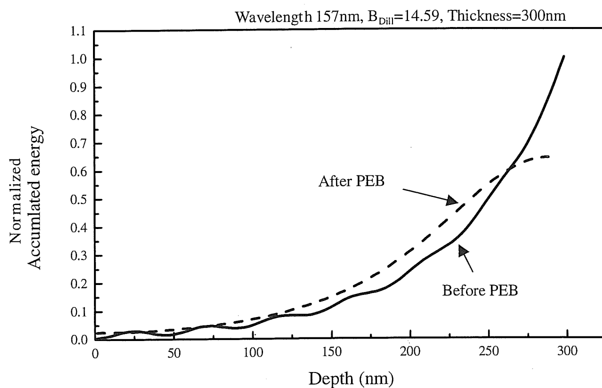

Fig. 6. Comparison of normalized accumulated energy in depth direction for after PEB and before PEB.

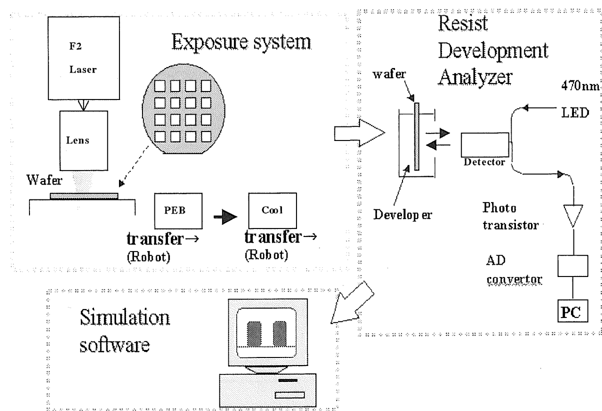

Fig. 7. The flow chart of analysis.

previous section, the theoretical distribution of accumulated energy in the resist film due to exposure can be determined (with calculations taking PEB into account) (Fig. 6). The accumulated energy value is thought to be proportional to the acid concentration [H^+] from photo acid generator (PAG). If the depth-direction accumulated energy distribution is integrated with respect to the resist depth, the average accumulated energy can be obtained. And if both these calculations are performed for different exposure doses, the relation between the average accumulated energy and the average development rate can be obtained. By applying this to Mack's development rate equation (original Mack's equation),[9] the relation between accumulated energy and development rate can be found. Furthermore, this equation can be used to convert the depth-direction accumulated energy distribution as seen in Figure 6 into a development rate distribution, enabling calculation of the development rate $R(E, Z)$ at different depths in the resist film for different exposure doses. Here, R is the development rate, E is the exposure dose, and Z is the depth in the resist. This method employs the Dill B parameter, thus even for F_2 exposure where development irregularity means thin film interference cannot be obtained, it is still possible to predict the development rate taking into account the effect of absorption in the resist film.

2.3 *Lithography simulation unit*

The lithography simulation unit adopts FINLE's PROLITH/2 (Positive Resist Optical LITHography model).[10] This software is capable of simulating the basic steps of lithography, including focusing, resist exposure (generation of photoacids), PEB-induced deprotection reactions, and development, to calculate the final resist profile. Optical intensities can be calculated based on scalar diffraction theory using the extended source method. This method determines the optical intensity resulting from a projection optical system with partial coherence and with limited diffraction and aberration, taking defocusing effects into account. Corrections for high numerical aperture (NA) are also performed, to more faithfully reproduce the effects of defocusing in the resist film.

Initially, the photoacid distribution induced in the resist film by exposure is calculated. That is, Dill's A, B and C parameters[5] are used to convert the optical intensity distribution in the film into a photoacid concentration distribution. Then, PEB-induced secondary photoacid diffusion is calculated, and dissociation of protection groups due to catalytic action of the acid is computed. The acid loss function of the photoacid can also be included in calculations. Development calculations are performed by converting the concentration distribution of the protection groups thus obtained into a development rate distribution using the development parameters. Through this series of calculations, the final resist profile is obtained. The calculation model used here is called a physical calculation model.

However, in many chemically amplified resists bleaching does not occur (parameter $A = 0$), making it difficult to determine the Dill A parameter.[9] In F_2 excimer laser exposure, there are no changes in transmittance due to exposure, as shown in Fig. 4, and the A parameter cannot be calculated. Hence in this system, instead of using the A and C parameters and the development parameters, the exposure energy and development rate data $R(E, Z)$ are used directly to calculate the development rate distribution from the optical intensity distribution within the film, thus performing measurement-based simulations to calculate development data.[10] Thus it is possible to perform simulations without calculating the Dill A and C parameters, development parameters, deprotection reaction parameters, or other parameters necessary for physical-model simulation. Furthermore, the $R(E, Z)$ data table used here takes into account the effect of absorption in the resist film with the use of the Dill B parameter, and this method introduces the principle of calculations used in physical-model simulations, in to a new type of model which merges physical-model simulation and measured-value simulation. Using this method, it is possible to simulate new lithography processes for which a model has not yet been established, such as F_2 excimer laser exposure. This method includes the PED effect[12] and other factors, thus making possible simulations that more nearly approximate actual conditions.

Using the above three process analysis units, it is possible to perform sample exposure, development rate analysis, and simulations to quickly assess F_2 excimer laser processes. Figure 7 illustrates the flow of processing from exposure to simulation.

3. Experimental

3.1 *Development analysis*

A positive chemically amplified (CA) resist for use with ArF excimer lasers, and a negative CA resist for use with electron beams, were employed in experiments using this system for F_2 excimer laser exposure, development analysis, and

Table I. Simulation conditions.

Positive chemically amplified resist for ArF excimer lasers exposure.	
Resist	PAR-101 (Sumitomo Chem.) ($n = 1.78$)
Thickness	303.5 nm
Pre-Bake	90°C, 90 s
PEB	100°C, 90 s
Substrate	Si without BARC ($n = 0.478$ $k = 2.000$)
B_{Dill}	14.59 (Measured by VUVES-4500 at 100 nm thickness)
Diffusion coefficient	46.7 nm^2/s
Negative chemically amplified resist for electron beam exposure.	
Resist	SAL-601 (Shipley) ($n = 1.80$)
Thickness	205.0 nm
Pre-Bake	90°C, 90 s
PEB	100°C, 90 s
Substrate	Si without BARC ($n = 0.478$ $k = 2.000$)
B_{Dill}	12.07 (Measured by VUVES-4500 at 100 nm thickness)
Diffusion coefficient	48.4 nm^2/s

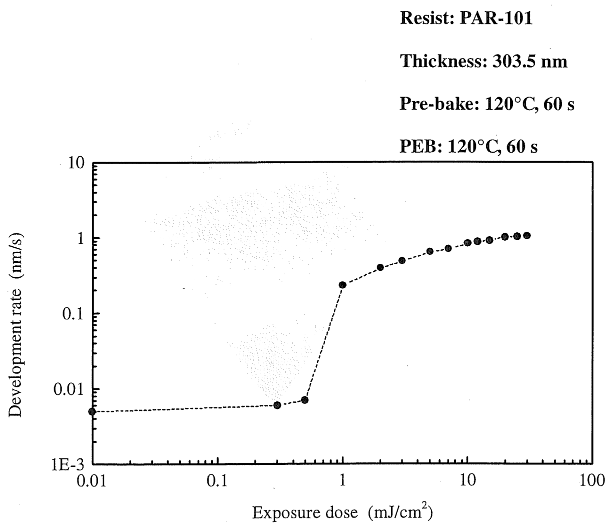

(a) PAR-101

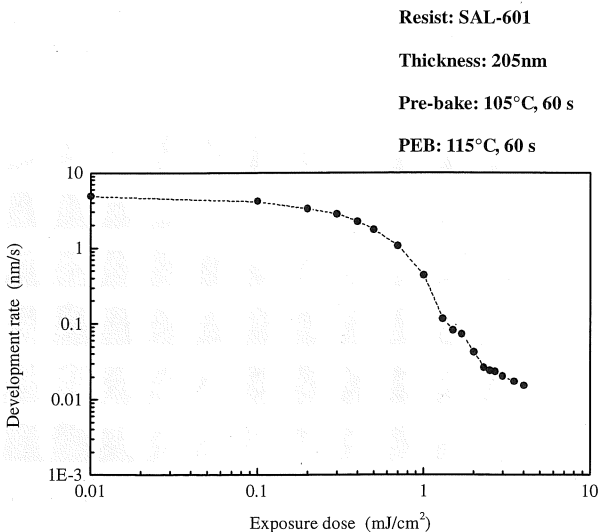

(b) SAL-601

Fig. 8. Exposure dose-Development rate curves for (a) PAR-101 and (b) SAL-601.

simulations. Table I shows the experimental conditions. In both cases, development involved dipping in NMD-3 (TMAH 2.38%). Figure 8(a) shows the discrimination curve for development of PAR-101 after exposure to F_2 excimer laser light. Here the exposure dose was varied between 0 mJ/cm^2 and 30 mJ/cm^2. PAR-101 is the sample for which F_2 excimer laser exposure does not yield adequate contrast $\tan\theta = 1.20$. Here $\tan\theta$ represents the rise angle of the discrimination curve; the higher its value, the higher the resist contrast. There is thought to be a correlation between $\tan\theta$ and the resolution limit, and it is believed that patterning is possible when $\tan\theta = 3$ or greater.[13] Figure 8(b) shows the discrimination curve for development of SAL-601 after F_2 excimer laser exposure. SAL-601 is a resist intended for electron beam exposure, but was found to afford sufficient contrast for patterning ($\tan\theta = -3.9$) upon F_2 excimer laser exposure as well. Figure 9 compares γ values for 60-s development of each of the resists (except for PAR-101 exposed to F_2 excimer laser light, developed for 200 s). Table II compares development characteristics of the two resists for F_2 exposure.

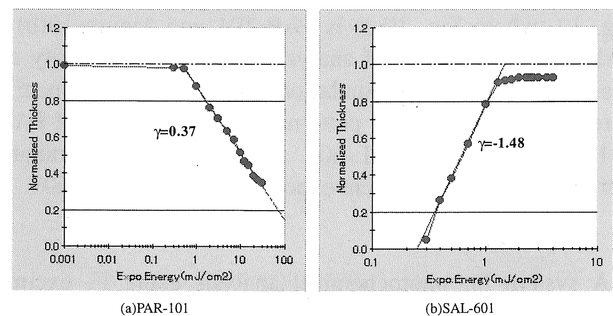

Fig. 9. Contrast curve for (a) PAR-101 and (b) SAL-601.

Table II. Comparison of development characteristics values at F_2 exposure.

	E_{th} (mJ/cm^2)	γ	$\tan\theta$	Development time (s)
PAR-101	32	0.37	1.20	200
SAL-601	0.56	−1.48	−3.9	60

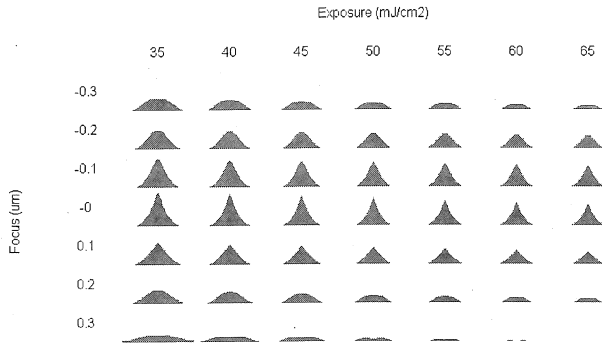

(a) PAR-101(Thickness=304nm; Development time=200s)

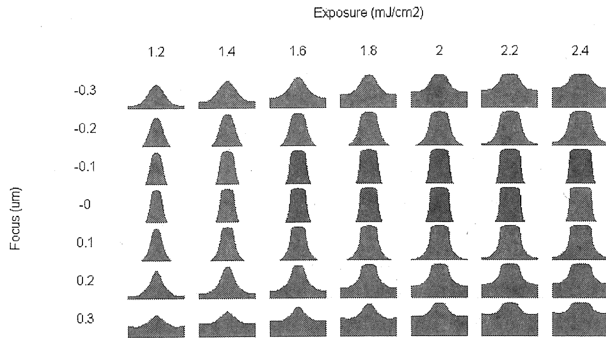

(b) SAL-601 (Thickness=205nm; Development time=60s)

Fig. 10. PROLITH/2 simulations showing the focus exposure matrix on 0.15 μm lines (NA = 0.7, σ = 0.6, wavelength = 157 nm) of (a) PAR-101 and (b) SAL-601.

3.2 *Profile simulations*

The exposure wavelength was 157 nm; the irradiation system coherence factor was taken to be 0.6. Line and space widths were 150 nm, and defocusing was assumed to be from -0.3 to $+0.3\,\mu$m.

The calculated development rate data $R(E, Z)$ resulting from F_2 excimer laser exposure of both resists was input in to the simulator, and profile calculations were performed for a 150 nm line pattern. The calculation results are shown in Fig. 10, where Fig. 10(a) is PAR-101 and Figure 10(b) is SAL-601. The results of analysis of the mask linearity appear in Figure 11. The simulation results reveal that linearity is retained for line-space patterns down to 130 nm for PAR-101, and 100 nm for SAL-601. Figure 12 shows simulated resolution limits at different exposure doses for SAL-601.

4. Conclusions

A system for photochemical analysis using F_2 excimer laser light, VUVES-4500, was developed. Using this system, 150 nm pattern profiles resulting from exposure of a positive resist for ArF excimer lasers and a negative resist for electron beam exposure to F_2 excimer laser light were studied. It was confirmed that this system can be applied even to resists with strong absorption. Hence when studying resist materials for F_2 excimer lasers for which a simulation model has not yet been established, in addition to optimizing the baking conditions, film thickness and development conditions, it should also be possible to expeditiously analyze the limits of resolution when using off-axis illumination exposure techniques.

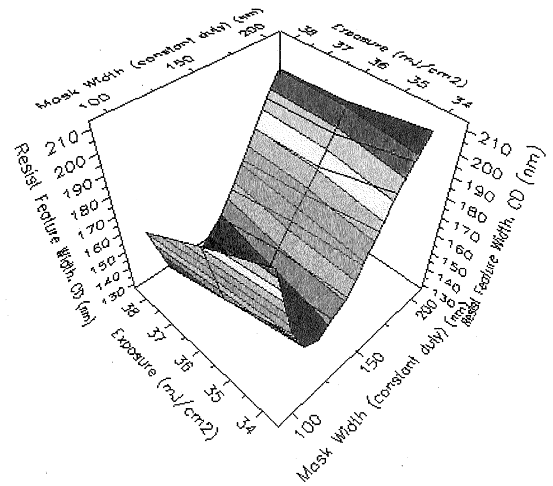

(a)PAR-101 (Thickness=304nm; Development time=200s)

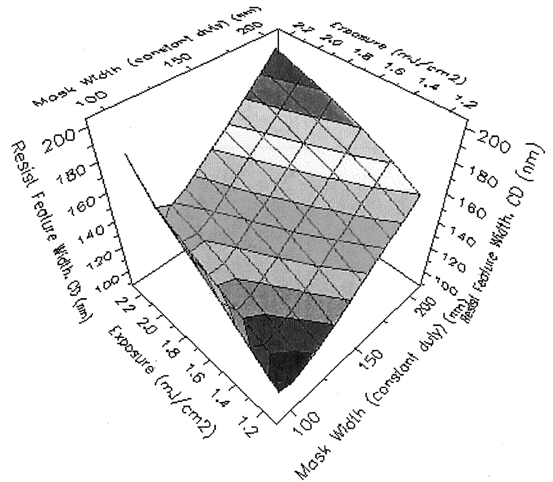

(b)SAL-601 (Thickness=205nm; Development time=60s)

Fig. 11. PROLITH/2 simulations showing the mask linearity (NA = 0.7, σ = 0.6, wavelength = 157 nm) of (a) PAR-101 and (b) SAL-601.

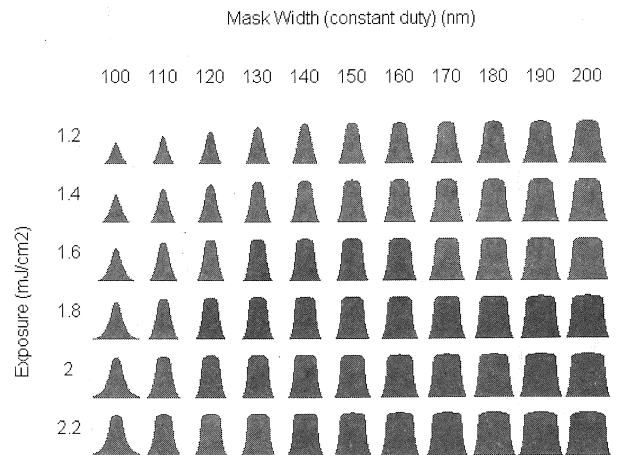

Fig. 12. PROLITH/2 simulations showing the resolution limit for SAL-601 (NA = 0.7, σ = 0.6, wavelength = 157 nm).

Acknowledgements

The authors are grateful to Mr. Itoh of the Optical Systems Research Laboratory in for help with the system design, and to Senior Researcher Dr. Uetani of Sumitomo Chemical and Mr. Kawabata of Shipley Far East for providing resist samples.

1) V. Pol, J. H. Bennevitz, G. C. Escher, M. Feldam, V. A. Firton, T. E. Jewell, B. E. Wilcomb and J. T. Clemens: Proc. SPIE **633** (1986) 186.
2) A. Sekiguchi, M. Kadoi, Y. Minami and T. Matsuzawa: Semiconductor World **6** (1997) 25.
3) Y. Uetani and K. Fujishima: Soc. Polym. Sci. Jpn. **8** (1999) 9.
4) F. Murai, J. Yamamoto, H. Yamaguchi and S. Okazaki: J. Vac. Sci. Technol. B **12** (1994) 3874.
5) F. H. Dill, W. P. Hornberger, P. S. Hauge and J. M. Shaw: IEEE Trans. Electron Devices **22** (1975) 445.
6) A. Sekiguchi, C. A. Mack, Y. Minami and T. Mastuzawa: Proc. SPIE **2725** (1996) 49.
7) F. H. Dill, A. R. Neureuther, J. A. Tuttle and E. J. Walker: IEEE Trans. Electron Devices **22** (1975) 456.
8) T. Ushirogouchi, T. Naito, K. Asakawa, N. Shida, M. Nakase and T. Tada: ACS Symp. Ser. **16** (1995) 240.
9) A. Sekiguchi, M. Kadoi, T. Matsuzawa and Y. Minami: Electron. & Commun. Jpn. Pt. 2 **82** (1999) 30.
10) Y. Minami and Sekiguchi: Electron. & Commun. Jpn. Pt. 2 **J76** (1993) 562 [in Japanese].
11) C. A. Mack, M. J. Maslow, R. Carpio and A. Sekiguchi: Olin Microelectron. Materials Inter Face '97 Proc. (1997) p. 203.
12) T. Ohfiji, A. G. Timko, O. Nalamasu and D. R. Stone: Proc. SPIE **1925** (1993) 213.
13) A. Sekiguchi, Y. Minami and Y. Sensu: Electrochem. Soc. Jpn. **42** (1992) 149.